

Synthesis of fluorinated oxadiazoles with gelation and oxygen storage ability†

Antonio Palumbo Piccionello,*^a Annalisa Guarcello,^a Alessandro Calabrese,^{a,b} Ivana Pibiri,^a Andrea Pace^a and Silvestre Buscemi^a

Received 2nd December 2011, Accepted 15th February 2012

DOI: 10.1039/c2ob07024c

A new family of fluorinated low molecular weight (LMW) gelators has been synthesized through SNAr substitution of 5-polyfluoroaryl-3-perfluoroheptyl-1,2,4-oxadiazoles with glycine ester. The obtained compounds give thermal and pH-sensitive hydrogels or thermo-reversible organogels in DMSO. Oxygen solubility studies showed the ability to maintain high oxygen levels in solution and in gel blend with plate counter agar (PCA).

Introduction

Gel formation represents an attractive research area due to the unique properties of this type of soft material which presents many applications in the biomedical field.¹ Hydrogels represent the most interesting class of gels due to their current and prospective pharmacological uses.¹ Compared to the most common polymeric gelators, which predominantly form chemical gels, low molecular weight gelators (LMWGs) essentially form physical gels in which the molecules are self-assembled into three-dimensional structures, held together by non-covalent interactions.² Because of the typical supramolecular interaction, these molecules are arranged as well ordered assemblies and the formed gels are stable, thermally reversible and exhibit a high tolerance towards additives.² Moreover, low minimal gelation concentrations (MGC) are often found for LMWGs.^{2e-g} In this context, the introduction of fluorinated moieties into amphiphilic molecules has been widely studied due to their peculiar properties such as chemical inertness, thermal stability, very high surface activity, high gas solubility and low critical micelle concentrations (CMC).^{3,4} Moreover, fluorinated colloidal systems allow the obtainment of highly organized structures such as micelles, bilayers, vesicles and tubules, whose formation is enhanced by the aggregation of fluorinated moieties.⁴ This tendency to self-assemble has been also used in order to promote hydrogel formation from various fluorinated polymers.⁵ Recently, we reported the introduction of fluorinated moieties into polyaspartamide copolymers using 3-perfluoroheptyl-5-

pentafluorophenyl-1,2,4-oxadiazole as arylating agent.⁶ Interestingly, the obtained fluorinated polymers formed association colloids consisting of macromolecular units where the hydrophobic fluorinated oxadiazole blocks were aggregated within the core of the micelle.⁶ Indeed, 1,2,4-oxadiazoles present many biological activities⁷ and their perfluoroalkylated derivatives possess a pronounced tendency to self-assemble.⁸ Based on these considerations, we decided to design new fluorinated amphiphilic oxadiazoles, with potential self-assembly and hydrogelation ability. In fact, while fluorinated LMW organogelators are common,⁹ only a few examples of fluorinated LMW hydrogelators have been reported.¹⁰ Additionally, the presence of functional groups able to respond to different acidic conditions has been considered due to the importance of pH-sensitive hydrogels.¹¹ According to the general structural architecture reported for low molecular weight hydrogelators,¹² our designed compounds contain a seven-carbon perfluoroalkyl chain as hydrophobic portion, a polyfluorophenyl-1,2,4-oxadiazole rigid spacer, and the aminoacidic moiety of glycine as a pH-sensitive polar head group (Fig. 1).

Results and discussion

Considering that 5-polyfluorophenyl-1,2,4-oxadiazoles can easily undergo nucleophilic aromatic substitution of the 4'-fluoro moiety under mild experimental conditions,¹³ we decided to

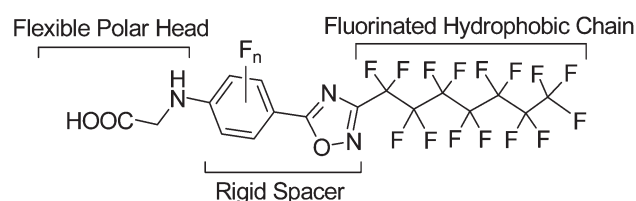


Fig. 1 General structure for designed fluorinated amphiphilic oxadiazoles.

^aDipartimento di Scienze e Tecnologie Molecolari e Biomolecolari – Sez. Chimica Organica “E. Paternò”, Università degli Studi di Palermo, Viale delle Scienze – Parco d’Orleans II, Ed. 17, I-90128 Palermo, Italy. E-mail: antonio.palumbopiccionello@unipa.it; Fax: +39091596825; Tel: +3909123897544

^bENEA UTTRI-RIF, Ufficio di Palermo, via Catania 2, 90141 Palermo, Italy

† Electronic supplementary information (ESI) available: NMR spectra of compounds 4–9. See DOI: 10.1039/c2ob07024c

introduce the aminoacidic moiety of glycine on the already formed oxadiazoles **4** during the late steps of the synthetic route (Scheme 1). In turn, 1,2,4-oxadiazoles **4** were obtained following the conventional *amidoxime route*⁷ through initial acylation of perfluoroheptylamidoxime **1**⁴ and subsequent solvent-free cyclization of the corresponding *O*-acyl-amidoxime **3** (Scheme 1). Glycine ethyl ester was then introduced through S_NAr , in DMF at rt, producing compounds **5**, which were finally converted into the corresponding acids **6** (Scheme 1).

Compounds **6a–c**, which differ in the fluorine content of the rigid spacer, resulted insoluble in water even after prolonged reflux. Nevertheless, complete dissolution of **6a–c** in water was reached by adding an equimolar amount of an inorganic base MOH ($M^+ = Li^+, Na^+, K^+$). Interestingly, gelation was observed after heating and subsequently cooling the obtained solutions, with formation of semi-transparent hydrogels from all compounds **6**. On the other hand, any attempt to obtain organogels from compounds **6** in common organic solvents failed due to formation of solutions (in DMF, DMSO, EtOH, MeOH, or THF) or precipitate (in DCM, $CHCl_3$, or $PhCH_3$). Minimal gelation concentrations (MGC, $mg\ mL^{-1}$) in water were determined by performing the tube inversion test on lithium, sodium and potassium salts of oxadiazoles **6a–c** (Table 1).

It is noteworthy that the fluorine content of the aryl spacer has a dramatic effect on the MGC which decreases by about 20–35% for each added fluorine atom and indicates the deprotonated form of **6c** as the most effective gelator in all cases. Considering the effect of cations on the gelation ability of compounds **6**, it's noteworthy that the MGC increased as the radius of the alkaline metal ion decreased. In this case K^+ , which compared with Li^+ and Na^+ has been recently shown to be the least effective in stabilizing spherical micelles of amphiphilic polycarboxylates,¹⁵ was the most efficient cation in enhancing

water gelation ability of deprotonated **6c**. A likely explanation considers the ability of the potassium cation in stabilizing aggregates with low curvature such as bilayers of cylindrical micelles.^{15,16}

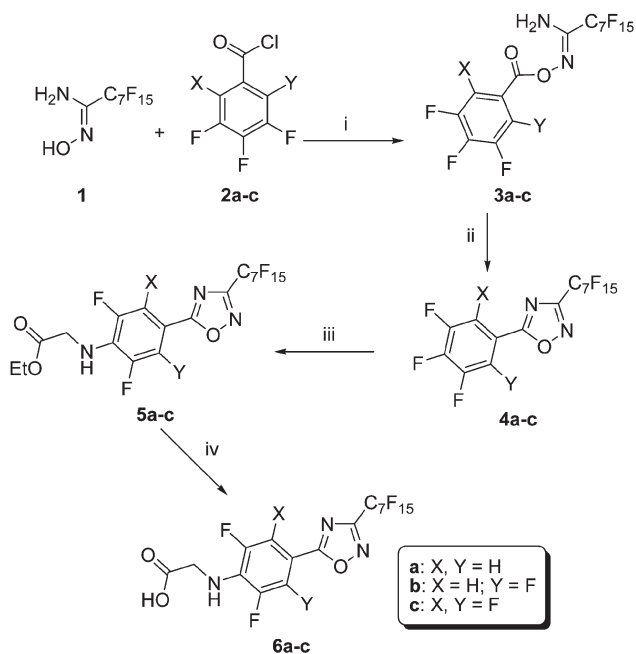
The self-assembling properties of the potassium salt of compound **6c** were further characterized by determining the critical aggregation concentration (CAC). By using pyrene as fluorescent probe, a CAC of $1.91 \pm 0.02 \times 10^{-4}\ M$ was found, a value which is about two orders of magnitude lower than that of other fluorinated anionic surfactants,^{10d} and than MGC. This result suggests the hierarchical self-assembly of aggregates toward the formation of physical gels. The pyrene emission I_1/I_3 ratio decreases as the concentration of **6c**⁻ increases, reaching its lowest value of 1.36 (Fig. 2) which is similar to that found for other fluorinated surfactants.¹⁷ This indicates that pyrene is presumably positioned at the interface of the hydrated aggregate palisade layer.¹⁷

All obtained gels from **6a–c** were stable at room temperature for more than two months and were responsive to pH and temperature changes. Addition of 1 equivalent of HCl to the gel phase caused precipitation of the oxadiazole compound while gel formation was again observed by addition of a base (Fig. 3). In particular, for the potassium salts of oxadiazole **6c**, a transition pH value of $pH_{sol-gel} = 6.6$ was determined for the gel disassembling process.

This reversible pH-dependent gelation behavior can be obviously ascribed to the presence of the glycine moiety.¹⁸ Similarly, liquid and gel phases were reversibly observed upon heating and cooling, respectively (Fig. 3). The gel–sol transition

Table 1 Minimal gelation concentration (MGC) in water for the anions of compounds **6a–c** with different cations

Compound	Cation	MGC ($mg\ mL^{-1}$)
6a	K^+	25
6a	Na^+	30
6a	Li^+	37.5
6b	K^+	20
6b	Na^+	22.5
6b	Li^+	30
6c	K^+	12.5
6c	Na^+	15
6c	Li^+	20



Scheme 1 Synthesis of compounds **5** and **6**. (i) K_2CO_3 , acetone, rt; (ii) $180\ ^\circ C$ /solvent-free (70–74% over two steps); (iii) glycine ethyl ester, K_2CO_3 , DMF, rt (65–86%); (iv) KOH, H_2O –THF, rt (77–95%).

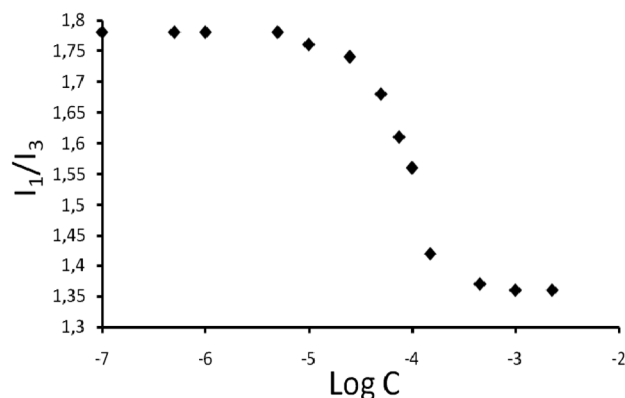


Fig. 2 Variations of the I_1/I_3 ratio of the pyrene vibronic fluorescence spectrum as a function of K^+6c^- concentration in water.

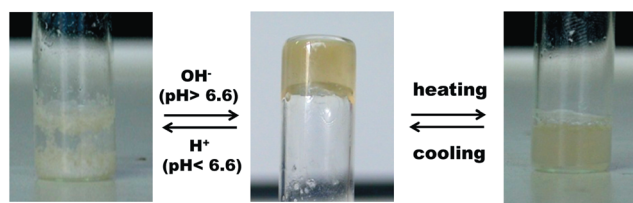


Fig. 3 Reversible sol-gel phase transition for the gel of **6c** triggered by pH and temperature.

Table 2 Gel-sol transition temperature (T_{gs}) for the anion of compound **6c** with different cations

Compound	Cation	T_{gs} (°C)
6c	K ⁺	26.7 ± 0.2
6c	Na ⁺	26.5 ± 0.2
6c	Li ⁺	27.6 ± 0.2

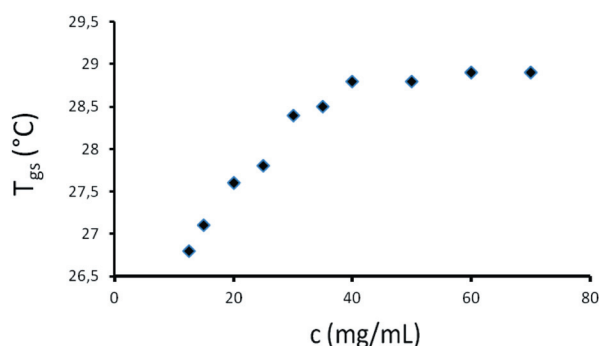


Fig. 4 Dependence of T_{gs} on the concentration of K⁺**6c**⁻ hydrogel.

temperatures (T_{gs}) of gels, at the MGC, obtained from compound **6c** with different cations are reported in Table 2. No significant variation of T_{gs} was observed by varying the alkaline metal.¹⁹ The gel-sol transition temperature (T_{gs}) of representative potassium salt of compound **6c** was also studied as a function of the gelator concentration, by using the dropping ball method (Fig. 4).

The T_{gs} increased by about 2.0 °C by increasing the concentration of the gelator from 12.5 to 70 mg mL⁻¹, without further significant changes at higher concentrations. Such a narrow T_{gs} variation indicates that the gel phase consists of an homogeneous micro-structured network.²⁰ Unfortunately, such a narrow variation and the lack of melting temperature of the potassium salt of **6c**, did not allow us to apply Schrader's equation²¹ to estimate the transition enthalpy.

POM images, obtained for the hydrogel of the potassium salt of **6c**, revealed the formation of a lamellar morphology (Fig. 5).

The morphology of xerogels obtained from compound **6c** was also studied by scanning electronic microscopy (SEM) as a function of the cations. A lamellar microstructure with the fluorinated amphiphile forming oriented porous planar sheet aggregates of 10–20 μm length was observed with potassium as the cation. Less ordered planar sheet aggregates a few micrometers in length were observed with sodium (Fig. 6).²² Such molecular arrangement could be interpreted as the initial formation of

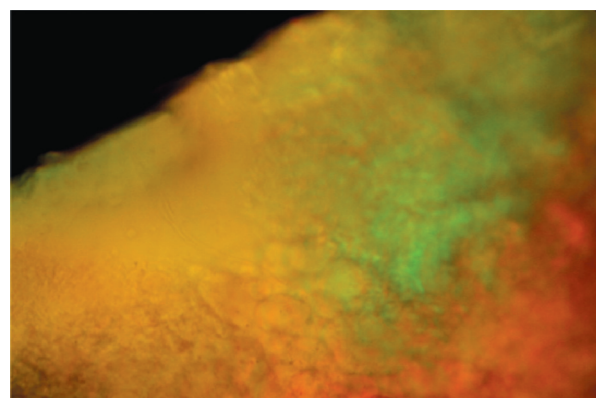


Fig. 5 POM image for gel obtained from compound **6c** as potassium salt.

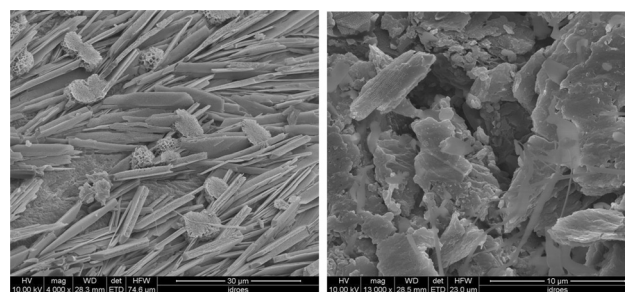


Fig. 6 SEM images for the xerogel obtained from compound **6c** as potassium salt (left) and as sodium salt (right).

Table 3 MGC and T_{gs} in DMSO for compounds **5a–c**

Compound	MGC (mg mL ⁻¹)	T_{gs} (°C)
5a	15	67.3 ± 0.2
5b	—	—
5c	10.5	30.6 ± 0.2

supramolecular aggregates with low curvature (for example a bilayer) and subsequent hierarchical self-assembly into lamellae. This hypothesis is in agreement with the ability of potassium ion to stabilize such supramolecular aggregates.^{15,16}

Additionally, the potential organogelation ability of esters **5a–c** was investigated in different solvents. Any attempt to obtain organogels from compounds **5** in common organic solvents failed due to formation of solutions (in DMF, EtOH, MeOH, THF, DCM, CHCl₃, PhCH₃). On the other hand, oxadiazoles **5a, c** form stable and semi-transparent organogels in DMSO, while compound **5b** results insoluble in the same solvent. This could be ascribed to the strongest lateral dipole moment induced by the asymmetric distribution of fluorine atoms on the phenyl-ring in **5b** with respect to **5a,c**.²³ Minimal gelation concentrations (MGC, mg mL⁻¹) in DMSO were determined by performing the tube inversion test (Table 3). Also in this case, the fluorine content on the phenyl-ring is crucial on the MGC values, revealing compound **5c**, with the highest fluorine content, as the most effective organogelators. Obtained organogels are stable for more than one month and exhibit a thermal responsive behavior.

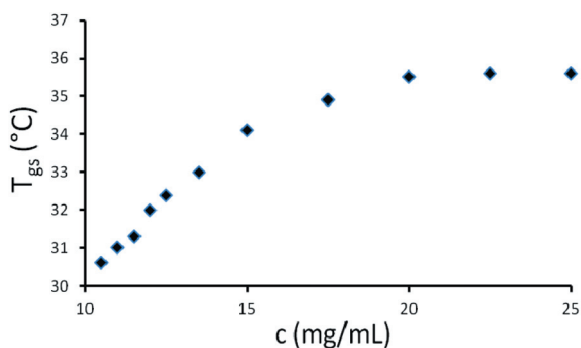


Fig. 7 Dependence of T_{gs} on the concentration of **5c** organogel in DMSO.

In fact, liquid and gel phases were reversibly observed upon heating and cooling, respectively. The gel–sol transition temperature (T_{gs}) of gels, at the MGC, obtained from compounds **5a** and **5c** were determined by using the dropping ball method and are reported in Table 3.

The gel–sol transition temperature (T_{gs}) of representative compound **5c** was also studied as a function of the gelator concentration (Fig. 7). Also in this case, a narrow increase of the T_{gs} (5 °C) was observed by increasing the concentration of the gelator from 10.5 to 25 mg mL⁻¹, without further significant changes at higher concentrations.

The gel–sol phase transition can be considered as a dissolution process of microcrystals and is described by eqn (1) derived from Schrader's relation:²¹

$$\ln C = -\Delta H_{gs}/RT_{gs} + \Delta H_{gs}/RT_m \quad (1)$$

where C is the molar gel concentration, ΔH_{gs} is the gel–sol transition enthalpy, R is the gas constant, T_{gs} is the transition temperature and T_m is the melting temperature of the pure compound. Therefore, an estimate of ΔH_{gs} for the organogel **5c** in DMSO was determined from the linear fitting of $\ln C$ for **5c** versus $1000/T_{gs}$ (Fig. 8).

Data analysis showed a good agreement between the value of ΔH_{gs} obtained from the slope ($\Delta H_{gs} = 77.5 \pm 0.8$ kJ mol⁻¹) and that obtained from intercept ($\Delta H_{gs} = 81 \pm 3$ kJ mol⁻¹) of the fitting equation.

POM images, obtained for the organogel in DMSO of **5c**, revealed the formation of a fibrillar network (Fig. 9). In this case such supramolecular architecture could be ascribed to the initial formation of cylindrical aggregates as previously observed for non-ionic fluorinated gelators.^{9,10}

For comparison, we also synthesized compounds **8** and **9** containing a longer C–H hydrophobic chain. These compounds were obtained, adapting the above described synthetic method, starting from 5-pentafluorophenyl-3-undecyl-1,2,4-oxadiazole **7** (Scheme 2).

Interestingly, the replacement of the perfluorocarbon moiety with a hydrocarbon chain strongly affected the aggregation behaviour. In fact, no gel formation was observed either for compound **8** in DMSO or for the potassium salt of compound **9** in H₂O, up to a 50 mg ml⁻¹ concentration. This suggests a crucial role of the perfluoroalkyl-chain for the supramolecular aggregation of these type of LMWGs.

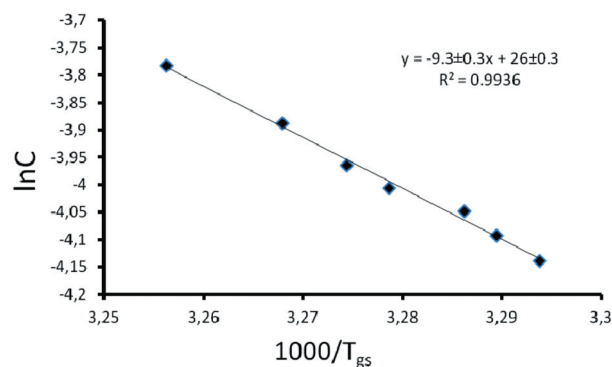


Fig. 8 Plot of the natural logarithm of **5c** concentration ($\ln C$) versus the reciprocal absolute temperature of gel–sol transition ($1000/T_{gs}$).

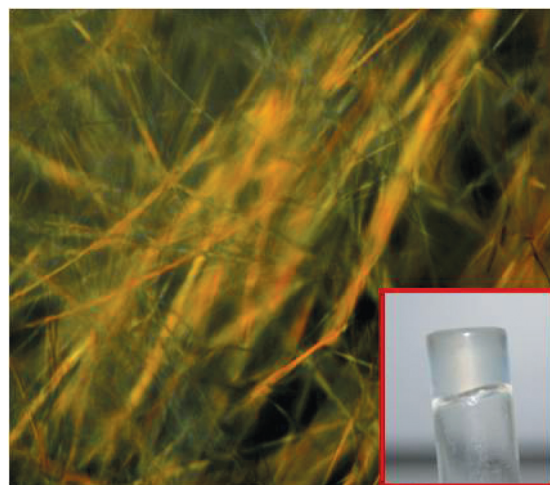
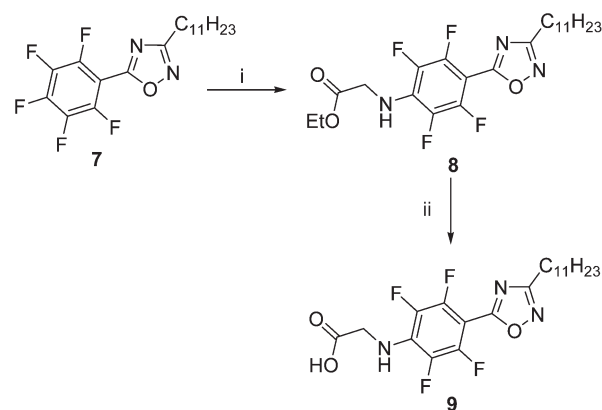


Fig. 9 POM image of organogel of compound **5c** in DMSO; image of the organogel (inset).



Scheme 2 Synthesis of compounds **8** and **9**. (i) glycine ethyl ester, K₂CO₃, DMF, rt (85%); (ii) KOH, H₂O–THF, rt (91%).

An interesting application of these fluorinated LMWGs can be envisaged by considering the oxygen affinity of perfluorocarbon moieties.⁴ Therefore, we decided to investigate if the occurrence of micellar aggregates formation, for representative compound **6c**, could exploit its potential as oxygen delivery system. In

order to obtain some information about the behavior as O_2 carriers, oxygen release kinetics from solutions of potassium salts of **6c** were performed, by means of a previously reported saturation method,⁶ at 25 °C and at different concentrations of K^+6c^- (10^{-4} and 10^{-3} M). Oxygen release studies in solutions, were also performed by using potassium perfluorooctanoate (**KPO**) as reference. **KPO** is a fluorinated anionic surfactant, which forms micelles at a concentration two orders of magnitude higher than K^+6c^- ($\sim 10^{-2}$ M), but does not form gels. Oxygen solubility was determined after saturation of the solutions ($pO_2 = 1$ atm) and monitored, as a function of time, at atmospheric pressure ($pO_2 = 0.21$ atm). According to reported *in vivo* kinetics experiments,²⁴ the obtained desaturation curves were approximated by a single exponential function (eqn (2))

$$[O_2] = [O_2]_0 + [O_2]_{\text{load}} \times e^{-Kt} \quad (2)$$

where $[O_2]_0$ (mg l^{-1}) is the oxygen solubility after saturation of the medium at t_0 , $[O_2]_\infty$ (mg l^{-1}) is the oxygen solubility at t_∞ , $[O_2]_{\text{load}} = [O_2]_0 - [O_2]_\infty$ represents the amount of oxygen loaded by the aggregate, and K (min^{-1}) is the clearance constant, *i.e.* the inverse of the rate of oxygen release from the medium.

The obtained data are reported in Table 4 and in Fig. 10.

At 10^{-4} M concentration, a value below the CAC of both **KPO** and K^+6c^- , the latter was able to dissolve more oxygen at saturation ($\Delta[O_2]_0 = 4.61$ ppm) and maintaining it in solution for a longer time than **KPO**. Moreover, O_2 solubility at saturation for K^+6c^- was also higher than in water ($\Delta[O_2]_0 = 2.21$ ppm) despite the low concentration of K^+6c^- . Oxygen solubility at atmospheric pressure ($[O_2]_\infty$) was slightly higher than in pure water for both **KPO** and K^+6c^- , with an higher value for **KPO**. At 10^{-3} M, where only compound K^+6c^- is above its CAC, K^+6c^- is able to dissolve more oxygen at atmospheric pressure than **KPO** and release it more than four times slower. The significant difference between K values of K^+6c^- and **KPO** at 10^{-3} M concentration, can be explained in terms of formation of micellar aggregates that allow K^+6c^- to create an oxygen reservoir, as previously observed for fluorinated polymeric amphiphiles.^{6b}

In this context, application of fluorinated compounds to dissolve respiratory gases has attracted significant interest focused primarily on their use to enhance oxygen supply to cells and tissues.²⁶ Therefore, the ability of salt K^+6c^- to maintain high oxygen level in solution prompted us to investigate the potential use of compound **6c** as oxygen transporter in cell culture systems.

Table 4 Parameters of eqn (2) determined for desaturation curves as a function of time of oxygen saturated aqueous solutions of **6c** and **PO**^a

Compound	10^{-4} M	10^{-3} M
6c	$[O_2]_0 = 40.66$ ppm	$[O_2]_0 = 37.38$ ppm
	$[O_2]_\infty = 8.55$ ppm	$[O_2]_\infty = 9.53$ ppm
	$K = 1.23 \times 10^{-2} \text{ min}^{-1}$	$K = 5.85 \times 10^{-3} \text{ min}^{-1}$
KPO	$[O_2]_0 = 36.05$ ppm	$[O_2]_0 = 41.27$ ppm
	$[O_2]_\infty = 8.83$ ppm	$[O_2]_\infty = 9.35$ ppm
	$K = 1.64 \times 10^{-2} \text{ min}^{-1}$	$K = 2.56 \times 10^{-2} \text{ min}^{-1}$

^a For pure water $[O_2]_0 = 38.45$ ppm,^{6b} $[O_2]_\infty = 8.37$ ppm.²⁵

The oxygen release curves were recorded at 37 °C as a function of time for both a plate counter agar (PCA) 1% (w/v) gel, used as model cell culture medium, and a PCA 1% (w/v) gel containing a 0.1% (w/v) of compound **6c** as additive (Fig. 11).

Interestingly, the addition of oxadiazole **6c** results in an improvement of the oxygen profile with respect to PCA gel.

Conclusions

In summary, new 1,2,4-oxadiazoles containing fluorinated hydrophobic chains and rigid spacers linked to an aminoacidic polar group, were synthesized and characterized as hydrogelators. They form thermally reversible and pH-sensitive gels with low MGC, if compared to similar fluorinated gelators.¹⁰ The

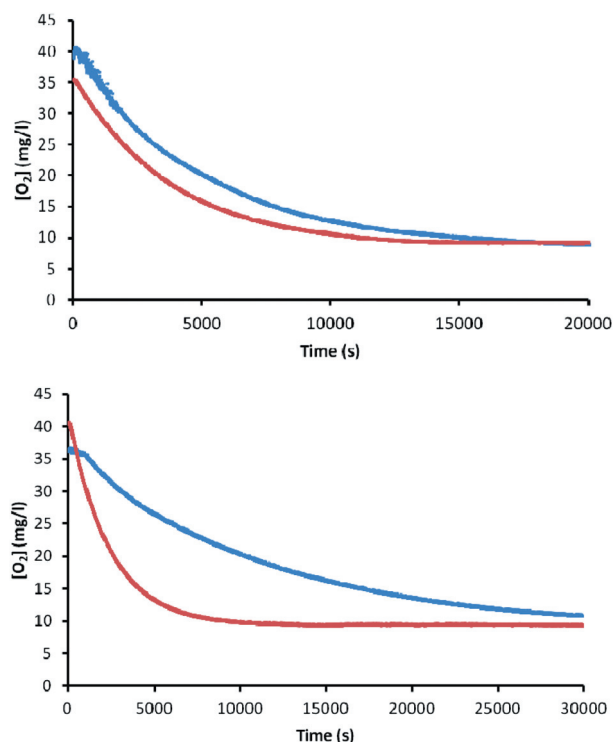


Fig. 10 Oxygen release curves from aqueous solutions of **6c** (blue) and **PO** (red) at 10^{-4} M (upper) and 10^{-3} M (lower).

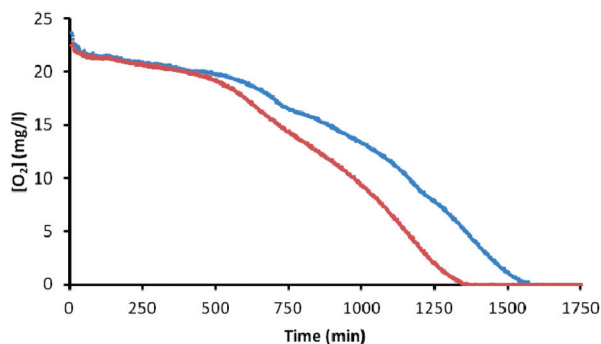


Fig. 11 Oxygen release curves from gels of PCA 1% (red) and PCA 1% + **6c** 0.1% (blue).

trend of the minimal gelation concentration, as a function of the structure of deprotonated **6a–c**, showed that the fluorine content of the aromatic portion is crucial for the gelation process highlighting the role of the fluoroaryl group in non-covalent interactions. The gelator **6c** forms, in water, ordered lamellar structures due to layered supramolecular assembly. The variation on MGC values could be interpreted in terms of the enhanced aggregation ability with potassium salts due to the formation of highly ordered structures in comparison with sodium salts as evidenced by SEM experiments. The obtained compounds may represent a new family of fluorinated LMWGs. The low clearance constant value for compound **6c** suggests the potential use as oxygen carrier. Further investigation on factors affecting the aggregation mode and on biomedical perspective applications are currently under way.

Experimental section

Instrumentation and chemicals

Melting points were determined on a hot-stage apparatus. FT-IR spectra were registered in Nujol mull. ¹H-NMR and ¹³C-NMR spectra were recorded at indicated frequencies, residual solvent peak was used as reference. Flash chromatography was performed by using silica gel (0.040–0.063 mm) and mixtures of ethyl acetate and petroleum ether (fraction boiling in the range of 40–60 °C) in various ratios. Compounds **1**,¹⁴ **3c**,¹⁴ **4c**¹⁴ and undecyl amidoxime²⁷ were obtained according to previously reported method.

General procedure for the synthesis of oxadiazoles **4a–b** and **7**

1.2 eq. of benzoyl chloride **2** (2.8 mmol) and K₂CO₃ (0.386 g, 2.8 mmol) were added to a solution of **1** or undecyl amidoxime²⁷ (2.33 mol) in acetone (50 mL). The mixture was stirred at room temperature for 1 h. The solvent was then removed under vacuum, the residue treated with water and a white solid was isolated by filtration. Obtained powder was heated at 180 °C in a tube until complete consumption of the starting material (TLC). The obtained residue was chromatographed producing oxadiazoles **4a–b** and **7**.

5-(3,4,5-Trifluorophenyl)-3-perfluoroheptyl-1,2,4-oxadiazole 4a. (0.98 g, 74%) mp 36–37 °C (from petroleum ether) (Found: C, 31.70; H, 0.30; N, 4.90. C₁₅H₂F₁₈N₂O requires C, 31.71; H, 0.35; N, 4.93%; ν_{\max} (Nujol)/cm⁻¹ 1632; δ_{H} (300 MHz; CDCl₃) 7.78–7.83 (m, 2H, Ar); δ_{C} (62.5 MHz; CDCl₃) 105–124 (overlapped signals, C₇F₁₅ + Ar), 143.6 (dt, ¹J_{C-F} = 261 Hz, ²J_{C-F} = 15 Hz, C–F Ar), 151.8 (dd, ¹J_{C-F} = 253 Hz, ²J_{C-F} = 8 Hz, C–F Ar), 162.5 (t, ²J_{C-F} = 28 Hz, Het C3) and 175.3 (Het C5); *m/z*: 568 (M⁺,100%).

5-(2,3,4,5-Tetrafluorophenyl)-3-perfluoroheptyl-1,2,4-oxadiazole 4b. (0.95 g, 70%) mp 28–29 °C (from petroleum ether) (Found: C, 30.70; H, 0.15; N, 4.80. C₁₅HF₁₉N₂O requires C, 30.74; H, 0.17; N, 4.78%; ν_{\max} (Nujol)/cm⁻¹ 1637; δ_{H} (300 MHz; CDCl₃) 7.86–7.89 (m, 1H, Ar); δ_{C} (62.5 MHz; CDCl₃) 104–120 (overlapped signals, C₇F₁₅ + Ar), 141.8 (dt, ¹J_{C-F} = 255 Hz, ²J_{C-F} = 13 Hz, C–F Ar), 144.6 (dt, ¹J_{C-F} = 264 Hz, ²J_{C-F} = 13 Hz, C–F

Ar), 147.1 (dd, ¹J_{C-F} = 263 Hz, ²J_{C-F} = 11 Hz, C–F Ar), 148.5 (dd, ¹J_{C-F} = 241 Hz, ²J_{C-F} = 9 Hz, C–F Ar), 162.3 (t, ²J_{C-F} = 28 Hz, Het C3) and 172.9 (Het C5); *m/z*: 586 (M⁺,100%).

5-(2,3,4,5,6-Pentafluorophenyl)-3-undecyl-1,2,4-oxadiazole 7. (0.71 g, 78%) oil (Found: C, 58.55; H, 5.95; N, 7.30. C₁₉H₂₃F₅N₂O requires C, 58.46; H, 5.94; N, 7.18%; ν_{\max} (Nujol)/cm⁻¹ 1657; δ_{H} (250 MHz; CDCl₃) 0.86 (t, 3H, ³J_{H-H} = 6.6 Hz, CH₃), 1.25–1.42 (m, 16H, overlapped signals), 1.74–1.86 (m, 2H, CH₂) and 2.82 (t, 2H, ³J_{H-H} = 7.6 Hz, Het–CH₂); δ_{C} (62.5 MHz; CDCl₃) 14.0 (CH₃), 22.6 (CH₂), 26.0 (CH₂), 26.9 (CH₂), 29.1 (CH₂), 29.2 (CH₂), 29.3 (CH₂), 29.4 (CH₂), 29.6 (2 × CH₂), 31.9 (CH₂), 101.5 (C–Het Ar), 138.1 (d, ¹J_{C-F} = 255 Hz, C–F Ar), 143.7 (d, ¹J_{C-F} = 260 Hz, C–F Ar), 145.5 (d, ¹J_{C-F} = 272 Hz, C–F Ar), 165.7 (Het C3) and 171.6 (Het C5); *m/z*: 390 (M⁺,100%).

General procedure for preparation of oxadiazoles **5a–c** and **8**

t-BuOK (0.448 g, 4 mmol) and, after 30 minutes, oxadiazole **4** or **7** (2 mmol) were added to a solution of glycine ethyl ester hydrochloride (0.558 g, 4 mmol) in DMF (3 mL). The reaction mixture was stirred at room temperature, until complete conversion of the starting material occurred (TLC). The mixture was then treated with water (50 mL) and extracted with EtOAc. The combined organic layers were dried over Na₂SO₄, filtered and the solvent removed under reduced pressure. The residue was chromatographed giving compound **5a–c** and **8**.

Ethyl 2-(2,6-difluoro-4-(3-perfluoroheptyl-1,2,4-oxadiazol-5-yl)phenylamino)acetate 5a. (0.85 g, 65%) mp 132–133 °C (from petroleum ether) (Found: C, 35.00; H, 1.50; N, 6.40. C₁₉H₁₀F₁₇N₃O₃ requires C, 35.04; H, 1.55; N, 6.45%; ν_{\max} (Nujol)/cm⁻¹ 3393, 1736 and 1624; δ_{H} (300 MHz; CDCl₃) 1.38 (t, ³J_{H-H} = 6.6 Hz, 3H, CH₃), 4.31–4.39 (m, 4H, CH₂O + CH₂N), 4.95 (bs, 1H, exch. with D₂O, NH) and 7.74 (dd, 2H, ³J_{H-F} = 7.8 Hz, ⁵J_{H-F} = 2.4 Hz, Ar); δ_{C} (62.5 MHz; CDCl₃) 14.1 (CH₃), 46.4 (CH₂N), 61.8 (CH₂O), 104–124 (overlapped signals, C₇F₁₅ + Ar), 132.5 (t, ²J_{C-F} = 13 Hz, C–N Ar), 151.5 (d, ¹J_{C-F} = 241 Hz, C–F Ar), 162.3 (t, ²J_{C-F} = 25 Hz, Het C3), 170.2 (CO) and 175.3 (Het C5); *m/z*: 651 (M⁺,100%).

Ethyl 2-(2,3,6-trifluoro-4-(3-perfluoroheptyl-1,2,4-oxadiazol-5-yl)phenylamino)acetate 5b. (1.03 g, 77%) mp 105–106 °C (from petroleum ether) (Found: C, 34.15; H, 1.30; N, 6.25. C₁₉H₉F₁₈N₃O₃ requires C, 34.10; H, 1.36; N, 6.28%; ν_{\max} (Nujol)/cm⁻¹ 3377, 1732 and 1637; δ_{H} (300 MHz; CDCl₃) 1.33 (t, ³J_{H-H} = 6.9 Hz, 3H, CH₃), 4.27–4.34 (m, 4H, CH₂O + CH₂N), 5.01 (bs, 1H, exch. with D₂O, NH) and 7.60–7.67 (m, 1H, Ar); δ_{C} (62.5 MHz; CDCl₃) 14.2 (CH₃), 46.2 (CH₂N), 62.0 (CH₂O), 96.2 (C–Het Ar), 106–120 (overlapped signals, C₇F₁₅ + Ar), 131.9 (C–N Ar), 140.7 (dd, ¹J_{C-F} = 259 Hz, ²J_{C-F} = 13 Hz, C–F Ar), 147.1 (d, ¹J_{C-F} = 243 Hz, C–F Ar), 147.8 (dd, ¹J_{C-F} = 259 Hz, ²J_{C-F} = 13 Hz, C–F Ar), 161.8 (t, ²J_{C-F} = 27 Hz, Het C3), 170.1 (CO) and 174.2 (Het C5); *m/z*: 669 (M⁺,100%).

Ethyl 2-(2,3,5,6-tetrafluoro-4-(3-perfluoroheptyl-1,2,4-oxadiazol-5-yl)phenylamino)acetate 5c. (1.18 g, 86%) mp 94–96 °C (from petroleum ether) (Found: C, 33.20; H, 1.10; N, 6.15. C₁₉H₈F₁₉N₃O₃ requires C, 33.21; H, 1.17; N, 6.11%);

ν_{\max} (Nujol)/ cm^{-1} 3364, 1732 and 1649; δ_{H} (300 MHz, CDCl_3): δ = 1.40 (t, 3H, $^3J_{\text{H-H}}$ = 6.3 Hz, CH_3), 4.34–4.41 (m, 4H, $\text{CH}_2\text{O} + \text{CH}_2\text{N}$) and 5.21 (bs, 1H, exch. with D_2O , NH); δ_{C} (62.5 MHz; CDCl_3) 13.9 (CH_3), 46.0 (CH_2N), 62.1 (CH_2O), 91.1 (t, $^2J_{\text{C-F}}$ = 13 Hz, C–Het Ar), 104–124 (overlapped signals, C_7F_{15}), 132.2 (C–N Ar), 136.9 (dd, $^1J_{\text{C-F}}$ = 240 Hz, $^2J_{\text{C-F}}$ = 13 Hz, C–F Ar), 146.2 (dd, $^1J_{\text{C-F}}$ = 261 Hz, $^2J_{\text{C-F}}$ = 9 Hz, C–F Ar), 161.9 (t, $^2J_{\text{C-F}}$ = 28 Hz, Het C3), 169.7 (CO) and 170.6 (Het C5); m/z : 687 (M^+ , 100%).

Ethyl 2-(2,3,5,6-tetrafluoro-4-(3-undecyl-1,2,4-oxadiazol-5-yl)phenylamino)acetate 8. (0.80 g, 85%) mp 83–85 °C (from petroleum ether) (Found: C, 58.40; H, 6.55; N, 8.90. $\text{C}_{23}\text{H}_{31}\text{F}_4\text{N}_3\text{O}_3$ requires C, 58.34; H, 6.60; N, 8.87%); ν_{\max} (Nujol)/ cm^{-1} 3372, 1726 and 1656; δ_{H} (300 MHz; CDCl_3) 0.89 (t, 3H, $^3J_{\text{H-H}}$ = 6.7 Hz, CH_3), 1.27–1.35 (m, 19H, overlapped signals), 1.76–1.86 (m, 2H, CH_2), 2.83 (t, 2H, $^3J_{\text{H-H}}$ = 7.6 Hz, Het– CH_2), 4.26–4.33 (m, 4H, $\text{CH}_2\text{O} + \text{CH}_2\text{N}$) and 4.96 (bs, 1H, exch. with D_2O , NH); δ_{C} (75 MHz; CDCl_3) 14.5 (2 × CH_3), 23.1 (CH_2), 26.5 (CH_2), 27.4 (CH_2), 29.5 (CH_2), 29.6 (CH_2), 29.7 (CH_2), 29.9 (CH_2), 30.0 (2 × CH_2), 32.3 (CH_2), 46.6 (CH_2N), 62.4 (CH_2O), 93.3 (t, $^2J_{\text{C-F}}$ = 14.1 Hz, C–Het Ar), 130.9–131.2 (m, C–N Ar), 137.3 (dd, $^1J_{\text{C-F}}$ = 238 Hz, $^2J_{\text{C-F}}$ = 14 Hz, C–F Ar), 146.1 (bd, $^1J_{\text{C-F}}$ = 252 Hz, C–F Ar), 167.9 (Het C3), 170.2 (CO) and 171.5 (Het C5); m/z : 473 (M^+ , 100%).

General procedure for preparation of compounds 6a–c

A solution of compound **5** or **8** (2 mmol) in THF (10 mL) and KOH 10 m (1 mL) was stirred at room temperature for 2 h. The reaction mixture was concentrated under reduced pressure, the residue was treated with water (25 mL) and the resulting mixture was acidified with HCl 1 m. The formed precipitate of compound **6a–c** or **9** was collected by filtration.

2-(2,6-Difluoro-4-(3-perfluoroheptyl-1,2,4-oxadiazol-5-yl)phenylamino)acetic acid 6a. (0.96 g, 77%) mp 139–140 °C (from H_2O) (Found: C, 32.70; H, 0.90; N, 6.70. $\text{C}_{17}\text{H}_6\text{F}_{17}\text{N}_3\text{O}_3$ requires C, 32.76; H, 0.97; N, 6.74%); ν_{\max} (Nujol)/ cm^{-1} 3410, 1732 and 1626; δ_{H} (300 MHz; DMSO-d_6) 4.17 (s, 2H, CH_2N), 6.89 (bs, 1H, exch. with D_2O , NH), 7.76 (bs, 2H, Ar) and 12.81 (bs, 1H, exch. with D_2O , OH); δ_{C} (62.5 MHz; DMSO-d_6) 45.5 (CH_2N), 105–120 (overlapped signals, $\text{C}_7\text{F}_{15} + \text{Ar}$), 131.8 (t, $^2J_{\text{C-F}}$ = 13 Hz, C–N Ar), 150.8 (d, $^1J_{\text{C-F}}$ = 240 Hz, C–F Ar), 161.0 (t, $^2J_{\text{C-F}}$ = 28 Hz, Het C3), 171.9 (CO) and 176.7 (Het C5); m/z : 623 (M^+ , 100%).

2-(2,3,6-Trifluoro-4-(3-perfluoroheptyl-1,2,4-oxadiazol-5-yl)phenylamino)acetic acid 6b. (1.06 g, 83%) mp 128–129 °C (from H_2O) (Found: C, 31.80; H, 0.80; N, 6.50. $\text{C}_{17}\text{H}_5\text{F}_{18}\text{N}_3\text{O}_3$ requires C, 31.84; H, 0.79; N, 6.55%); ν_{\max} (Nujol)/ cm^{-1} 3452, 1724 and 1639; δ_{H} (300 MHz; DMSO-d_6) 4.17 (bs, 2H, CH_2N), 7.18 (bs, 1H, exch. with D_2O , NH), 7.57–7.63 (m, 1H, Ar) and 12.90 (bs, 1H, exch. with D_2O , OH); δ_{C} (62.5 MHz; DMSO-d_6) 45.3 (CH_2N), 96.1 (C–Het Ar), 105–120 (overlapped signals, $\text{C}_7\text{F}_{15} + \text{Ar}$), 133.4 (C–N Ar), 139.4 (d, $^1J_{\text{C-F}}$ = 232 Hz, C–F Ar), 146.6 (d, $^1J_{\text{C-F}}$ = 236 Hz, C–F Ar), 147.3 (d, $^1J_{\text{C-F}}$ = 255 Hz, C–F Ar), 160.8 (t, $^2J_{\text{C-F}}$ = 28 Hz, Het C3), 171.7 (CO) and 174.1 (Het C5); m/z : 641 (M^+ , 100%).

2-(2,3,5,6-Tetrafluoro-4-(3-(perfluoroheptyl)-1,2,4-oxadiazol-5-yl)phenylamino)acetic acid 6c. (1.25 g, 95%) mp 127–130 °C (from H_2O) (Found: C, 30.90; H, 0.60; N, 6.35. $\text{C}_{17}\text{H}_4\text{F}_{19}\text{N}_3\text{O}_3$ requires C, 30.97; H, 0.61; N, 6.37%); ν_{\max} (Nujol)/ cm^{-1} 3394, 1722 and 1661; δ_{H} (300 MHz; DMSO-d_6) 4.16 (bs, 2H, CH_2N), 7.60 (bs, 1H, exch. with D_2O , NH) and 12.95 (bs, 1H, exch. with D_2O , OH); δ_{C} (62.5 MHz; DMSO-d_6) 46.0 (CH_2N), 88.2 (C–Het Ar), 103–120 (overlapped signals, C_7F_{15}), 133.9 (C–N Ar), 136.2 (d, $^1J_{\text{C-F}}$ = 246 Hz, C–F Ar), 145.8 (d, $^1J_{\text{C-F}}$ = 248 Hz, C–F Ar), 160.9 (t, $^2J_{\text{C-F}}$ = 28 Hz, Het C3), 171.1 (Het C5) and 171.9 (CO); m/z : 659 (M^+ , 100%).

2-(2,3,5,6-Tetrafluoro-4-(3-(undecyl)-1,2,4-oxadiazol-5-yl)phenylamino)acetic acid 9. (0.81 g, 91%) mp 110–112 °C (from H_2O) (Found: C, 56.60; H, 6.20; N, 9.30. $\text{C}_{21}\text{H}_{27}\text{F}_4\text{N}_3\text{O}_3$ requires C, 56.62; H, 6.11; N, 9.43%); ν_{\max} (Nujol)/ cm^{-1} 3354, 1734 and 1653; δ_{H} (300 MHz; CDCl_3) 0.88 (t, 3H, $^3J_{\text{H-H}}$ = 6.0 Hz, CH_3), 1.26–1.37 (m, 16H, overlapped signals), 1.78–1.83 (m, 2H, CH_2), 2.84 (t, 2H, $^3J_{\text{H-H}}$ = 7.8 Hz, Het– CH_2), 4.37 (bs, 2H, CH_2N) and 4.94 (bs, 1H, exch. with D_2O , NH); δ_{C} (75 MHz; CDCl_3) 12.8 (CH_3), 21.4 (CH_2), 24.7 (CH_2), 25.7 (CH_2), 27.8 (CH_2), 27.9 (CH_2), 28.0 (CH_2), 28.1 (CH_2), 28.3 (2 × CH_2), 30.6 (CH_2), 44.5 (CH_2N), 91.7 (m, C–Het Ar), 129.4 (m, C–N Ar), 135.6 (bd, $^1J_{\text{C-F}}$ = 230 Hz, C–F Ar), 144.5 (bd, $^1J_{\text{C-F}}$ = 256 Hz, C–F Ar), 166.3 (Het C3), 169.7 (Het C5) and 172.6 (CO); m/z : 445 (M^+ , 100%).

Gel formation and MGC determination

A weighed amount of gelator and solvent were placed in a vial. An equimolar amount of the inorganic base (KOH, NaOH or LiOH) was added for determinations with compounds **6a–c** in water. The mixture was heated at 50 °C until a clear solution was obtained. The vials were allowed to cool down to room temperature. The state of the solution was evaluated by inverting the vial. MGC was the minimal concentration which gave no liquid flow.

Fluorescence measurements

Fluorescence emission spectra were registered in water. Emission spectra were recorded in the range 350–500 nm using an excitation wavelength of 333 nm. The widths of the slits were set at 1.5 and 1.0 nm for excitation and emission, respectively. The mixtures for the measurements were prepared as following. Known amounts of a solution of pyrene in acetone were carefully added to dark flasks. After solvent evaporation, the sample solutions were added and equilibrated at room temperature for 2 days. For all of the mixtures, the final concentration of pyrene was 5×10^{-7} M (*i.e.*, its solubility in water).

Determination of $\text{pH}_{\text{sol-gel}}$

A gel of compound **6c**, above MGC concentration (15 mg mL^{-1}) was prepared in 10 mL of water, according to the general procedure described above. An initial pH = 9.8 was measured by submerging a pH-meter electrode within the gel phase. Equal amounts (11 μL , 0.05 eq.) of HCl 1 m were subsequently added

to the gel phase, which was heated and cooled after each acid addition observing solubilization (upon heating) and gel formation (upon cooling). A final pH = 6.6 was determined when the gel formation was no more occurring, after a total addition of 0.5 eq. of HCl.

Determination of T_{gs}

T_{gs} were determined through the dropping ball method. A steel ball (160 mg) was gently placed on the top of the gel (2 g) in a glass vial. The closed vial was placed firmly in a water bath, which was heated progressively at a rate of 0.1 °C per minute. The sample temperature was determined by a sensor dipped in a separate vial, next to the heating gel, which was filled with the same solvent. The T_{gs} was defined as the temperature at which the ball touched the bottom of the vial. The experiment was repeated three times to produce consistent results.

Scanning electron microscopy (SEM)

The morphology and the size of the aggregates obtained in aqueous phase have been observed by scanning electron microscopy (SEM). The samples have been prepared by putting the gels in a carbon stub and letting them dry at room temperature overnight before electron microscope analysis.

Oxygen solubility measurements

Oxygen solubility measurements were performed, as previously reported,⁶ by using a digital oxymeter, with a Schott Gerade 120 mm probe having a membrane with an exterior Teflon layer. Measures were recorded by placing the electrode tip into the bulk phase at 80 mm distance from the air–liquid (or air–gel) interface. Data from oxygen saturated aqueous solutions (20 ml) containing K^+6c^- or **KPO** at different concentrations, were taken at atmospheric pressure. In particular, each solution was initially stirred with a magnetic stir bar while pure oxygen was continuously bubbled. The temperature of each solution was adjusted to 25 °C by using a thermostated oil bath. Once the solution reached a stable maximum oxygen concentration (saturated solution), bubbling was stopped and the release of dissolved oxygen was determined by evaluating the change in the oxygen solubility (desaturation) as a function of time. Similarly, measurements on PCA and **6c@PCA** gels were performed at 37 °C, without stirring.

Acknowledgements

The authors are grateful to Dr Maria Luisa Bondi (ISMN-CNR, Division of Palermo) for SEM measurements. Financial support from the University of Palermo is gratefully acknowledged.

Notes and references

- (a) *Hydrogels in Medicine and Pharmacy*, ed. N. A. Peppas, CRC Press, Boca Raton, 1987, vol. 3; (b) K. Y. Lee and J. D. Mooney, *Chem. Rev.*, 2001, **101**, 1869; (c) J. Jagur-Grodzinski, *Polym. Adv. Technol.*, 2010, **21**, 27; (d) G. Pitarresi, G. Tripodo, R. Calabrese, E. F. Craparo, M. Licciardi and G. Giammona, *Macromol. Biosci.*, 2008, **8**, 891; (e) G. Tripodo, G. Pitarresi, G. Cavallaro, F. S. Palumbo and G. Giammona, *Macromol. Biosci.*, 2009, **9**, 393; (f) G. Tripodo, G. Pitarresi, F. S. Palumbo, E. F. Craparo and G. Giammona, *Macromol. Biosci.*, 2005, **5**, 1074.
- (a) P. Terech and R. G. Weiss, *Chem. Rev.*, 1997, **97**, 3133; (b) L. A. Estroff and A. D. Hamilton, *Chem. Rev.*, 2004, **104**, 1201; (c) M. de Loos, B. L. Feringa and J. H. van Esch, *Eur. J. Org. Chem.*, 2005, 3615; (d) N. M. Sangeetha and U. Maitra, *Chem. Soc. Rev.*, 2005, **34**, 821. As examples of gelators (supergelators) which gelate at very low concentration see: (e) H. Kobayashi, A. Friggeri, K. Koumoto, M. Amai, S. Shinkai and D. N. Reinhoudt, *Org. Lett.*, 2002, **4**, 1423; (f) A. Srivastava, S. Ghorai, A. Bhattacharjya and S. Bhattacharya, *J. Org. Chem.*, 2005, **70**, 6574; (g) Y. Qiao, Y. Lin, Z. Yang, H. Chen, S. Zhang, Y. Yan and J. Huang, *J. Phys. Chem. B*, 2010, **114**, 11725.
- (a) R. Filler, Y. Kobayashi and L. M. Yagupolskii, *Organofluorine Compounds in Medicinal Chemistry and Biomedical Applications*, Elsevier, Amsterdam, 1993; (b) *Chemistry of Organic Fluorine Compounds II. A Critical Review*, ed. M. Hudlicky and A. E. Pavlath, ACS Monograph 187, American Chemical Society, Washington, DC, 1995.
- See for example: (a) J. G. Riess, *Tetrahedron*, 2002, **58**, 4113; (b) M. P. Krafft, *Curr. Opin. Colloid Interface Sci.*, 2003, **8**, 213; (c) M. P. Krafft, *J. Polym. Sci., Part A: Polym. Chem.*, 2006, **44**, 4251.
- See for example: (a) J. Roovers, *Macromolecules*, 1986, **18**, 1361; (b) A. Matsuda, T. Kaneko, J. Gong and Y. Osada, *Macromolecules*, 2000, **33**, 2535; (c) K. Matsumoto, R. Nishimura, H. Mazaki, H. Matsuoka and H. Yamaoka, *J. Polym. Sci., Part A: Polym. Chem.*, 2001, **39**, 3751; (d) G. Tae, J. A. Kornfield, J. A. Hubbell, D. Johannsmann and T. E. Hogen-Esch, *Macromolecules*, 2001, **34**, 6409; (e) K. Kuroda, K. Fujimoto, J. Sunamoto and K. Akiyoshi, *Langmuir*, 2002, **18**, 3780; (f) A. F. M. Kilbinger and R. H. Grubbs, *Angew. Chem., Int. Ed.*, 2002, **41**, 1563; (g) W. F. Lee and T. M. Liu, *J. Appl. Polym. Sci.*, 2006, **100**, 4661.
- (a) D. Mandracchia, A. Palumbo Piccionello, G. Pitarresi, A. Pace, S. Buscemi and G. Giammona, *Macromol. Biosci.*, 2007, **7**, 836; (b) G. Pitarresi, A. Palumbo Piccionello, R. Calabrese, A. Pace, S. Buscemi and G. Giammona, *J. Fluorine Chem.*, 2008, **129**, 1096.
- For a recent review on 1,2,4-oxadiazoles see: A. Pace and P. Pierro, *Org. Biomol. Chem.*, 2009, **7**, 4337–4348.
- F. Lo Celso, I. Pibiri, A. Triolo, R. Triolo, A. Pace, S. Buscemi and N. Vivona, *J. Mater. Chem.*, 2007, **17**, 1201.
- See for example: (a) J. Loiseau, M. Lescanne, A. Colin, F. Fages, J.-B. Verlhac and J.-M. Vincent, *Tetrahedron*, 2002, **58**, 4049; (b) G. Mathew, S. L. Snyder, P. Terech, C. J. Glinka and R. G. Weiss, *J. Am. Chem. Soc.*, 2003, **125**, 10275; (c) M. George, S. L. Snyder, P. Terech and R. G. Weiss, *Langmuir*, 2005, **21**, 9970; (d) A. R. Borges, M. Hyacinth, M. Lum, C. M. Dingle, P. L. Hamilton, M. Chruszcz, L. Pu, M. Sabat and K. L. Caran, *Langmuir*, 2008, **24**, 7421; (e) S. S. Babu, V. K. Praveen, S. Prasanthkumar and A. Ajayaghosh, *Chem.–Eur. J.*, 2008, **14**, 9577; (f) A. Raghavanpil, S. Reinartz and K. W. Hutchenson, *J. Fluorine Chem.*, 2009, **130**, 410.
- (a) T. Imae, K. Funayama, M. P. Krafft, F. Giulieri, T. Tada and T. Matsumoto, *J. Colloid Interface Sci.*, 1999, **212**, 330; (b) S. F. Pang and D. B. Zhu, *Chem. Phys. Lett.*, 2002, **358**, 479; (c) A. Palumbo Piccionello, A. Pace, S. Buscemi, N. Vivona and G. Giorgi, *Tetrahedron Lett.*, 2009, **50**, 1472; (d) S. Buscemi, G. Lazzara, S. Milioto and A. Palumbo Piccionello, *Langmuir*, 2009, **25**, 13368; (e) D. M. Ryan, S. B. Anderson, F. Timur Senguen, R. E. Youngman and B. L. Nilsson, *Soft Matter*, 2010, **6**, 475; (f) G. Godeau, C. Brun, H. Arnion, C. Staedel and P. Barthélémy, *Tetrahedron Lett.*, 2010, **51**, 1012.
- (a) G. Giammona, G. Pitarresi, G. Cavallaro, B. Carlisi, E. F. Craparo and D. Mandracchia, *J. Drug Delivery Sci. Technol.*, 2006, **16**, 77; (b) M. A. Casadei, G. Pitarresi, R. Calabrese, P. Paolicelli and G. Giammona, *Biomacromolecules*, 2008, **9**, 43.
- T. Kunitake, Y. Okahata, M. Shimomura, S. Yasunami and K. Takarabe, *J. Am. Chem. Soc.*, 1981, **103**, 5401.
- (a) S. Buscemi, A. Pace, R. Calabrese, N. Vivona and P. Metrangolo, *Tetrahedron*, 2001, **57**, 5865; (b) A. Pace, I. Pibiri, S. Buscemi, N. Vivona and L. Malpezzi, *J. Org. Chem.*, 2004, **69**, 4108; (c) S. Buscemi, A. Pace, I. Pibiri, N. Vivona and T. Caronna, *J. Fluorine Chem.*, 2004, **125**, 165; (d) S. Buscemi, A. Pace, A. Palumbo Piccionello, I. Pibiri and N. Vivona, *Heterocycles*, 2005, **65**, 387; (e) A. Palumbo Piccionello, A. Pace, I. Pibiri, S. Buscemi and N. Vivona, *Tetrahedron*, 2006, **62**, 8792; (f) S. Buscemi, A. Pace, A. Palumbo Piccionello, S. Pappalardo, D. Garozzo, T. Pilati, G. Gattuso, A. Pappalardo, I. Pisagatti and M. F. Parisi, *Tetrahedron Lett.*, 2006, **47**, 9049; (g) A. Palumbo Piccionello, A. Pace, P. Pierro, I. Pibiri, S. Buscemi and N. Vivona, *Tetrahedron*,

- 2009, **65**, 119; (h) I. Pibiri, A. Palumbo Piccionello, A. Calabrese, S. Buscemi, N. Vivona and A. Pace, *Eur. J. Org. Chem.*, 2010, 4549.
- 14 S. Buscemi, A. Pace, A. Palumbo Piccionello and N. Vivona, *J. Fluorine Chem.*, 2006, **127**, 1601.
- 15 K. Rosenlehner, B. Schade, C. Böttcher, C. M. Jäger, T. Clark, F. W. Heinemann and A. Hirsch, *Chem.–Eur. J.*, 2010, **16**, 9544.
- 16 C. M. Jäger, A. Hirsch, B. Schade, C. Böttcher and T. Clark, *Chem.–Eur. J.*, 2009, **15**, 8586.
- 17 K. C. Hoang and S. Meozzi, *Langmuir*, 2004, **20**, 7347.
- 18 pK_a values could not be determined due to insolubility in water at $pH < pH_{sol-gel}$, see: A. Bryson, N. R. Davies and E. P. Serjeant, *J. Am. Chem. Soc.*, 1963, **85**, 1933.
- 19 As example of negligible effects of salts on T_{gs} , see: S. Kumar Kundu, M. Yoshida and M. Shibayama, *J. Phys. Chem. B*, 2010, **114**, 1541 and references cited therein.
- 20 J. Kowalczyk, S. Jarosz and J. Tritt-Goc, *Tetrahedron*, 2009, **65**, 9801.
- 21 K. Murata, K. Aoki, T. Suzuki, T. Hanada, H. Kawabata, T. Komori, F. Oseto, K. Ueda and S. Shinkai, *J. Am. Chem. Soc.*, 1994, **116**, 6664 and references cited therein.
- 22 As examples on the ions influence on the gel properties see: (a) H. Basit, A. Pal, S. Sen and S. Bhattacharya, *Chem.–Eur. J.*, 2008, **14**, 6534; (b) A. Pal, H. Basit, S. Sen, V. K. Aswal and S. Bhattacharya, *J. Mater. Chem.*, 2009, **19**, 4325.
- 23 M. Hird, *Chem. Soc. Rev.*, 2007, **36**, 2070.
- 24 B. A. Berkowitz, C. A. Wilson and D. L. Hatchell, *Invest. Ophthalmol. Vis. Sci.*, 1991, **32**, 2382.
- 25 P. C. Rooney and D. D. Daniels, *Pet. Technol. Q.*, 1998, **3**, 97.
- 26 K. C. Lowe, *J. Fluorine Chem.*, 2002, **118**, 19.
- 27 K. P. Flora, B. van't Riet and G. L. Wampler, *Cancer Res.*, 1978, **38**, 1291.